

October 31, 2018

Lifshitz Topological Black Holes

R.B. Mann*

Kavli Institute for Theoretical Physics, University of California, Santa Barbara, CA 93106,
USA

Abstract

I find a class of black hole solutions to a (3+1) dimensional theory gravity coupled to abelian gauge fields with negative cosmological constant that has been proposed as the dual theory to a Lifshitz theory describing critical phenomena in (2+1) dimensions. These black holes are all asymptotic to a Lifshitz fixed point geometry and depend on a single parameter that determines both their area (or size) and their charge. Most of the solutions are obtained numerically, but an exact solution is also obtained for a particular value of this parameter. The thermodynamic behaviour of large black holes is almost the same regardless of genus, but differs considerably for small black holes. Screening behaviour is exhibited in the dual theory for any genus, but the critical length at which it sets in is genus-dependent for small black holes.

PACS numbers: 11.25.Tq , 04.20.Jb, 04.20.Ha

Typeset Using L^AT_EX

*email: rbmann@sciborg.uwaterloo.ca; on leave from Department of Physics and Astronomy, University of Waterloo, Waterloo, Ontario, N2L 3G1, Canada

1 Introduction

The scope of concepts and applications of holography has blossomed in recent years. Realized in terms of the AdS/CFT correspondence, holography asserts that gravitational dynamics in an asymptotically Anti de Sitter (AdS) spacetime can be mapped onto a (relativistic) conformal field theory (CFT) in one less dimension [1]. This duality conjecture has proven to be a useful tool in understanding the behaviour of strongly interacting field theories, whose dual description is in terms of weakly coupled gravitational dynamics in a bulk spacetime that is asymptotically AdS.

Over the years holographic duality has been extended beyond high energy physics to a much broader class of spacetimes and dual physical systems. Some investigations have extended these ideas to asymptotically de Sitter [2] and asymptotically flat spacetimes [3], where holographic renormalization has been shown to be a fruitful tool for understanding conserved quantities and gravitational thermodynamics. More recently holography has been qualitatively employed in improving our understanding of transport properties of QCD quark-gluon plasmas [4] and in the construction of gravity models that are conjectured to be dual to various systems in atomic physics and condensed matter physics. For example holography has been shown to be applicable to a class of strongly correlated electron and atomic systems that exhibit relativistic dispersion relations, and whose dynamics near a critical point is well described by a relativistic CFT. The AdS/CMat correspondence is being actively employed to study superconductivity [5], the quantum Hall effect [6], and a number of other condensed matter systems that can be described by CFTs [7].

A key feature of interest is the scaling property

$$t \rightarrow \lambda^z t \quad \mathbf{x} \rightarrow \lambda \mathbf{x} \quad (1.1)$$

exhibited by fixed points governing the behaviour of various condensed matter systems. This behaviour differs from that which arises in the conformal group

$$t \rightarrow \lambda t \quad \mathbf{x} \rightarrow \lambda \mathbf{x} \quad (1.2)$$

and is concretely realized in the (2+1) dimensional theory

$$S = \int dt d^2 \mathbf{x} \left(\dot{\phi}^2 - K(\nabla \phi)^2 \right) \quad (1.3)$$

known as the Lifshitz theory. The action (1.3) is invariant under the scaling relation (1.1) with $z = 2$ and has been used to model quantum critical behavior in strongly correlated electron systems [8, 9].

From a holographic perspective the conjectured dual to this system is a gravitational theory [10] whose equations of motion yielded solutions with spacetime metrics asymptotic to the form

$$ds^2 = \ell^2 \left(-r^{2z} dt^2 + \frac{dr^2}{r^2} + r^2 d\mathbf{x}^2 \right) \quad (1.4)$$

where the coordinates (t, r, x^1, x^2) are dimensionless. These obey the scaling relations

$$t \rightarrow \lambda^z t \quad r \rightarrow \lambda^{-1} r \quad \mathbf{x} \rightarrow \lambda \mathbf{x} \quad (1.5)$$

and the only length scale in the geometry is ℓ . Metrics asymptotic to (1.4) can be generated as solutions to the equations of motion that follow from the action

$$S = \int d^4x \sqrt{-g} \left(R - 2\Lambda - \frac{1}{4} F_{\mu\nu} F^{\mu\nu} - \frac{1}{12} H_{\mu\nu\tau} H^{\mu\nu\tau} - \frac{C}{\sqrt{-g}} \epsilon^{\mu\nu\alpha\beta} B_{\mu\nu} F_{\alpha\beta} \right) \quad (1.6)$$

where $\epsilon^{\mu\nu\alpha\beta}$ is the Levi-Civita tensor density and $F_{\mu\nu} = \partial_{[\mu} A_{\nu]}$ and $H_{\mu\nu\tau} = \partial_{[\mu} B_{\nu\tau]}$ are Abelian gauge fields that are topologically coupled with coupling constant C . The quantity Λ is the cosmological constant. In order to obtain the asymptotic behaviour (1.4) these constants are given by [10]

$$\Lambda = -\frac{z^2 + z + 4}{2\ell^2} \quad 2z = (C\ell)^2 \quad (1.7)$$

in terms of the length scale ℓ .

Recently spherically symmetric solutions to the equations of motion that follow from (1.6) were obtained for the $z = 2$. These solutions included a discrete set of solutions known as Lifshitz stars as well as a continuous set of black hole solutions having finite temperature [11]. The purpose of this paper is to extend this work to the case of topological black holes, namely those whose event horizons are toroidal or of higher genus as a consequence of identifications made in the spacetime [12].

These black holes differ considerably from one another depending on the size of the event horizon, which is uniquely fixed in terms of their electric charge (or vice-versa). Large black holes have thermodynamic behaviour that is essentially the same regardless of the genus. However small black holes have markedly different genus-dependent thermodynamic behaviour. The entropy of genus-1 black holes scales linearly with the temperature for all values of the black hole radius. Higher genus black holes must have a radius $r_h > 1/\sqrt{5}$, with units defined as in eq. (1.4). As their radius decreases, so does their charge, and as $r_h \rightarrow 1/\sqrt{5}$ these black holes approach their extremal AdS counterparts [13] and have

the same asymptotic structure. While most solutions must be obtained numerically, it is possible to find an exact black hole solution in the higher-genus case. This solution appears to correspond to its zero-mass AdS counterpart, though its asymptotic behaviour is given by (1.4). Although all these results are for $z = 2$, generalization to higher z should be possible.

The solutions found here differ from those with obtained from gravity duals of other non-relativistic quantum systems [14], for which topological black hole solutions have also recently been found [15].

2 Lifshitz Asymptotics and Exact Solutions

The field equations that follow from the action (1.6) are

$$\nabla^\nu F_{\mu\nu} = -\frac{C}{6\sqrt{-g}}\epsilon_{\mu\nu\alpha\beta}H^{\nu\alpha\beta} \quad (2.1)$$

$$\nabla^\tau H_{\mu\nu\tau} = \frac{C}{2\sqrt{-g}}\epsilon_{\mu\nu\alpha\beta}F^{\alpha\beta} \quad (2.2)$$

$$G_{\mu\nu} - \frac{5}{\ell^2}g_{\mu\nu} = \frac{1}{2}\left(F_{\mu\tau}F_\nu^\tau - \frac{1}{4}g_{\mu\nu}F^2\right) + \frac{1}{4}\left(H_{\mu\sigma\tau}H_\nu^{\sigma\tau} - \frac{1}{6}g_{\mu\nu}H^2\right) \quad (2.3)$$

In order to solve these equations an ansatz is needed that preserves the basic symmetries under consideration. For the metric I shall take

$$ds^2 = \ell^2\left(-r^4 f^2(r)dt^2 + \frac{g^2(r)dr^2}{r^2} + r^2 d\Omega_k^2\right) \quad (2.4)$$

where

$$d\Omega_k^2 = \begin{cases} d\theta^2 + \sin^2\theta d\phi^2 & k = +1 \\ d\theta^2 + \theta^2 d\phi^2 & k = 0 \\ d\theta^2 + \sinh^2\theta d\phi^2 & k = -1 \end{cases} \quad (2.5)$$

is the metric for spatial sections at fixed (t, r) corresponding to the genus $\mathbf{g} = 0$ (spherical), $\mathbf{g} = 1$ (flat/toroidal), and $\mathbf{g} \geq 2$ (hyperbolic) cases. Compact spatial sections at fixed r are possible by making appropriate identifications in the \mathbf{x} coordinates [16, 17].

The gauge field strengths are

$$F_{rt} = -2\ell g(r)h(r)f(r)r \quad H_{r\theta\phi} = 2\ell^2 j(r)g(r)r \begin{cases} \sin\theta & k = +1 \\ \theta & k = 0 \\ \sinh\theta & k = -1 \end{cases} \quad (2.6)$$

with all other components either vanishing or being given by antisymmetrization.

The field strength $F_{\mu\nu}$ is that of an electric field directed radially outward, and described by the function $h(r)$ in an orthonormal basis. This field sources the 3-form field strength $H_{\mu\nu\tau}$ and vice-versa. This latter field is therefore electrically charged and corresponds to a charged fluid whose density is given by $j(r)$ in an orthonormal basis [11].

The field equations (2.1 – 2.3) reduce to the system

$$r \frac{df}{dr} = -\frac{5}{2}f(r) + \frac{1}{2}f(r)g(r)^2 \left(5 + \frac{k}{r^2} + j(r)^2 - h(r)^2 \right) \quad (2.7)$$

$$r \frac{dg}{dr} = \frac{3}{2}g(r) - \frac{1}{2}g(r)^3 \left(5 + \frac{k}{r^2} - j(r)^2 - h(r)^2 \right) \quad (2.8)$$

$$r \frac{dj}{dr} = 2g(r)h(r) + \frac{1}{2}j(r) - \frac{1}{2}j(r)g(r)^2 \left(5 + \frac{k}{r^2} + j(r)^2 - h(r)^2 \right) \quad (2.9)$$

$$r \frac{dh}{dr} = 2g(r)j(r) - 2h(r) \quad (2.10)$$

which is a system of ODEs that can be solved by standard numerical methods.

An exact solution to the above equations is

$$f(r) = j(r) = \sqrt{1 + \frac{k\ell^2}{2r^2}} \quad g(r) = \frac{1}{\sqrt{1 + \frac{k\ell^2}{2r^2}}} \quad h(r) = 1 \quad (2.11)$$

yielding the metric

$$ds^2 = \left(-\frac{r^2}{\ell^2} \left(\frac{r^2}{\ell^2} + \frac{k}{2} \right) dt^2 + \frac{dr^2}{\left(\frac{r^2}{\ell^2} + \frac{k}{2} \right)} + r^2 d\Omega_k^2 \right) \quad (2.12)$$

where I have rescaled $r \rightarrow r/\ell$ and $t \rightarrow t/\ell$. This solution is valid only for $z = 2$ and does not straightforwardly generalize to other values of $z > 1$.

The spacetime described by (2.12) is singular at $r = 0$ for all values of k . For $k = 0$ it becomes the metric (1.4): all its curvature scalars are finite but it is not geodesically complete. This kind of metric can be regarded as physically reasonable if there exists a regular black hole solution that approaches it in some extremal limit [10, 18]. For $k \neq 0$ the Kretschmann scalar diverges at $r = 0$. If $k = 1$ this is a naked singularity, but if $k = -1$ it is cloaked by an event horizon. Hence the metric

$$ds^2 = \left(-\frac{r^2}{\ell^2} \left(\frac{r^2}{\ell^2} - \frac{1}{2} \right) dt^2 + \frac{dr^2}{\left(\frac{r^2}{\ell^2} - \frac{1}{2} \right)} + r^2 (d\theta^2 + \sinh^2(\theta) d\phi^2) \right) \quad (2.13)$$

is an exact black hole solution to the field equations provided $h(r) = 1$ and $j(r) = \sqrt{1 - \frac{\ell^2}{2r^2}}$. The event horizon is located at $r = \ell/\sqrt{2}$. This metric would appear to be the analogue of

a zero-mass topological AdS black hole [13], though it should be noted that defining mass and other conserved charges in this theory remains an open question at this stage.

The asymptotic behaviour of the system (2.7)–(2.10) is the same for all values of k , and so its analysis is identical to the given for the $k = 1$ case [11]. Equations (2.8)–(2.10) form a closed system for the set $\{g(r), j(r), h(r)\}$ and can be considered separately; once they are solved then eq. (2.7) can be solved for $f(r)$. Linearization of these equations indicates that there is a zero mode at large r . However this mode must have zero amplitude if the system is to approach the Lifshitz metric (1.4). This can only happen if the initial values of the functions are appropriately adjusted (fine-tuned) to ensure that each function in the set $\{g(r), j(r), h(r)\}$ approaches unity.

3 Series and Numerical Black Hole Solutions

The system (2.7)–(2.10) can be solved both for large r and near the event horizon using series expansions. For large r the solution is

$$\begin{aligned}
f &= 1 + \frac{k}{4r^2} - \frac{k^2}{32r^4} + \left(\frac{k^3}{128} - \frac{kh_L}{12}\right) \frac{1}{r^6} + \left(\frac{13k^2h_L}{384} - \frac{5k^4}{2048} + \frac{15h_L^4}{64}\right) \frac{1}{r^8} \\
g &= 1 - \frac{k}{4r^2} + \left(\frac{h_L}{2} + \frac{3k^2}{32}\right) \frac{1}{r^4} - \left(\frac{5k^3}{128} + \frac{3kh_L}{8}\right) \frac{1}{r^6} + \left(\frac{7k^2h_L}{32} + \frac{35k^4}{2048} + \frac{3h_L^4}{32}\right) \frac{1}{r^8} \\
j &= 1 + \frac{k}{4r^2} - \left(\frac{3h_L}{2} + \frac{k^2}{32}\right) \frac{1}{r^4} + \left(\frac{k^3}{128} + \frac{7kh_L}{8}\right) \frac{1}{r^6} - \left(\frac{13k^2h_L}{32} + \frac{5k^4}{2048} + \frac{21h_L^4}{32}\right) \frac{1}{r^8} \\
h &= 1 + \frac{h_L}{r^4} - \frac{kh_L}{2r^6} + \left(\frac{7k^2}{32}h_L + \frac{7}{16}h_L^2\right) \frac{1}{r^8} \tag{3.1}
\end{aligned}$$

and is governed by one constant h_L , that parametrizes how rapidly the electric field falls off at large r . For $k = 0$ the falloff is very rapid, particularly for $f(r)$, whose subleading term is proportional to $1/r^8$.

It is also possible to solve the equations near the event horizon. Under the assumption that the black hole is not extremal, the metric functions g_{tt} and g_{rr} must respectively have a simple zero and a simple pole at the horizon $r = r_0$. The electric field $h(r_0) = h_0$ is assumed to be finite at $r = r_0$. Unlike the situation for the (AdS)-Reissner-Nordstrom metric, these values are not independent because of the presence of the charged fluid (the 3-form field strength). For a static configuration the gravitational pull of the black hole must balance the self-repulsion of the fluid, whose value must also vanish at the horizon if the electric field is finite there.

Writing $r = r_0 + x$, the resultant near-horizon series solution is

$$\begin{aligned}
f &= f_0\sqrt{x} (1 + f_1x + f_2x^2 + \dots) \\
g &= \frac{g_0}{\sqrt{x}} (1 + g_1x + g_2x^2 + \dots) \\
j &= j_0\sqrt{x} (1 + j_1x + j_2x^2 + \dots) \\
h &= h_0 (1 + h_1x + h_2x^2 + \dots)
\end{aligned} \tag{3.2}$$

where

$$\begin{aligned}
f_1 &= -\frac{5k^2 - 52r_0^4h_0^2 + 45kr_0^2 - 11kr_0^2h_0^2 + 6r_0^4h_0^4 + 100r_0^4}{2(r_0(k + 5r_0^2 - r_0^2h_0^2))^2} \\
g_0 &= \frac{r_0^{3/2}}{\sqrt{(k + 5r_0^2 - r_0^2h_0^2)}} \\
g_1 &= \frac{3k^2 - 24r_0^4h_0^2 + 25kr_0^2 - 7kr_0^2h_0^2 + 4r_0^4h_0^4 + 50r_0^4}{2r_0(k + 5r_0^2 - r_0^2h_0^2)^2} \\
j_0 &= 2\frac{\sqrt{r_0}h_0}{\sqrt{k + 5r_0^2 - r_0^2h_0^2}} \\
j_1 &= -\frac{h_0(k^2 + 11kr_0^2 - kr_0^2h_0^2 - 8r_0^4h_0^2 + 30r_0^4)}{2r_0(k + 5r_0^2 - r_0^2h_0^2)^2} \\
h_1 &= 2\frac{(k + 3r_0^2 - r_0^2h_0^2)}{(k + 5r_0^2 - r_0^2h_0^2)r_0}
\end{aligned} \tag{3.3}$$

with the remaining coefficients determined in terms of h_0 and r_0 .

From (3.3) it clear that the constraint

$$(5 - h_0^2)r_0^2 + k > 0 \tag{3.4}$$

must be respected so that the solutions are real. For $k = 0, 1$ this imposes an upper bound on $|h_0|$, whereas for $k = -1$ it imposes a lower bound of $r_0 > 1/\sqrt{5}$ on the size of the black hole.

Further progress can only be made numerically. Since the equations are all first order ODEs, the shooting method can be used to solve them. Choosing some value of r_0 for the black hole, one can then choose a value for h_0 and then find the initial values of the functions $g(r)$, $h(r)$, and $j(r)$ from the series solutions for some value of $r > r_0$. This becomes the initial data for the system (2.8)–(2.10), which can then be numerically solved. The value of $h(r)$ can be computed for $r = R \gg r_0$; should $|h(R) - 1| > \varepsilon$, where $\varepsilon \ll 1$ is some level of tolerance, then the process is repeated, with value of h_0 adjusted, until $|h(R) - 1| < \varepsilon$.

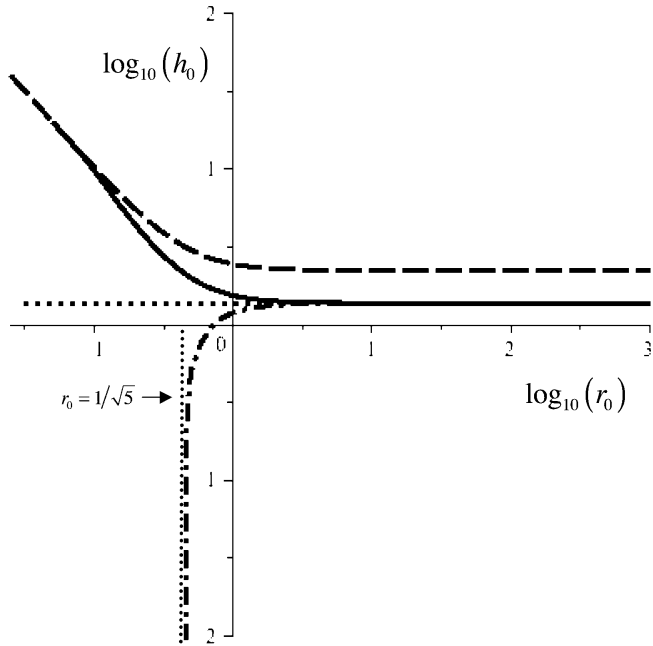


Figure 1: h_0 vs. r_0 on a log-log scale for spherical ($k = 1$, solid), toroidal ($k = 0$, dot) and higher-genus ($k = -1$, dot-dash) black holes. The limit given in eq. (3.4) for $k = 1$ is the dashed line. The intersection point of the $k = -1$ curve with the r_0 axis corresponds to the exact solution (2.13).

This then gives a black hole solution of radius r_0 with asymptotic behaviour given by the metric (1.4).

In practice it proves best to begin with large black holes, for which the value of h_0 remains constant. Numerically I find that setting $h_0 = 1.374$ yields valid solutions for $r_0 > 10$ for all values of k . For $k = 0$ this value of h_0 yields black hole solutions for all values of r_0 that were computationally viable. For $r_0 < 10$ it is necessary to systematically adjust the value of h_0 upward for $k = 1$ and downward for $k = -1$.

Figure 1 illustrates the behaviour of h_0 as a function of r_0 on a log-log plot. For $k = 1$, the value of h_0 asymptotes to the upper bound given in (3.4). The extremal limit appears to occur when the bound is saturated as $r_0 \rightarrow 0$; it does not appear to be possible to find series solutions for $r_0 > 0$ in the extremal case. For $k = -1$ the value of h_0 approaches zero as $r_0 \rightarrow 1/\sqrt{5}$. In this case the limit is evidently that of an extremal topological AdS black hole with genus $g > 2$. For the exact solution (2.13), $r_0 = 1/\sqrt{2}$ and $h_0 = h(r) = 1$,

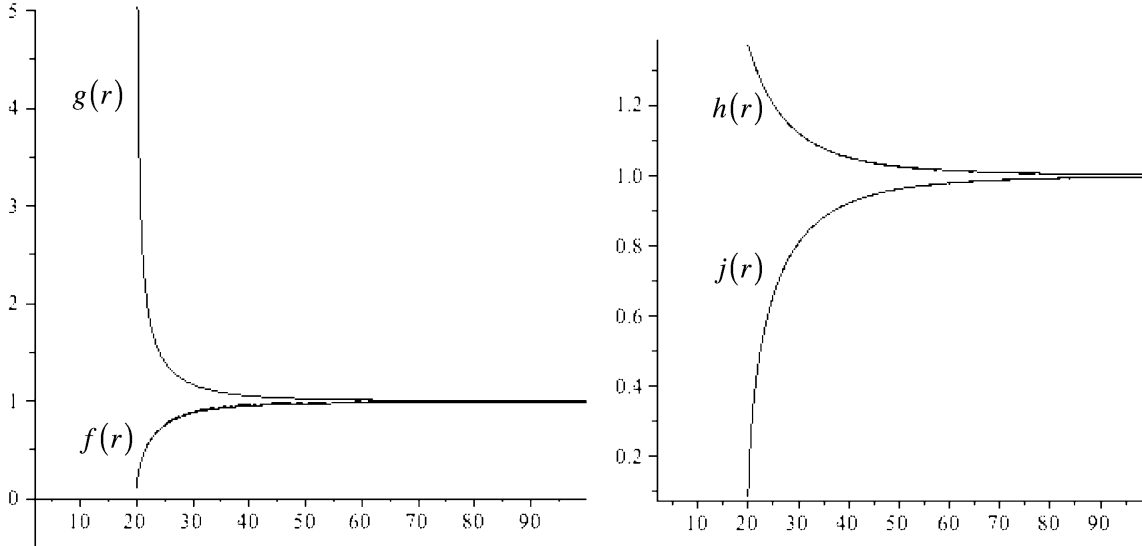


Figure 2: A plot of the metric and gauge functions for $r_0 = 20$ for all three values of k . The three curves overlap within the plotting resolution.

corresponding to the intersection point of the $k = -1$ curve with the r_0 in figure 1. The exact solution provides a useful check on the numerical solution, and it can be verified that the solutions for the metric and gauge functions are identical to within limits of tolerance (taken to be 10^{-4}).

The metric functions and gauge field strengths are essentially indistinguishable amongst the different values of k for $r_0 > 10$, as an example illustrates in figure 2. Small differences begin to appear for intermediate values of r_0 , as shown in figure 3, and for small r_0 the distinctions are quite significant, as depicted in figures 4 and 5.

4 Black Hole Thermodynamics

The temperature of Lifshitz black holes is easily evaluated using standard Wick-rotation methods, yielding the result

$$T = \frac{f_0 r_0^3}{4\pi g_0} = \frac{f_0 r_0^{3/2} \sqrt{-h_0^2 r_0^2 + k + 5r_0^2}}{4\pi} \quad (4.1)$$

where f_0 is dependent upon r_0 so that the metric has the asymptotic behaviour given in equation (1.4).

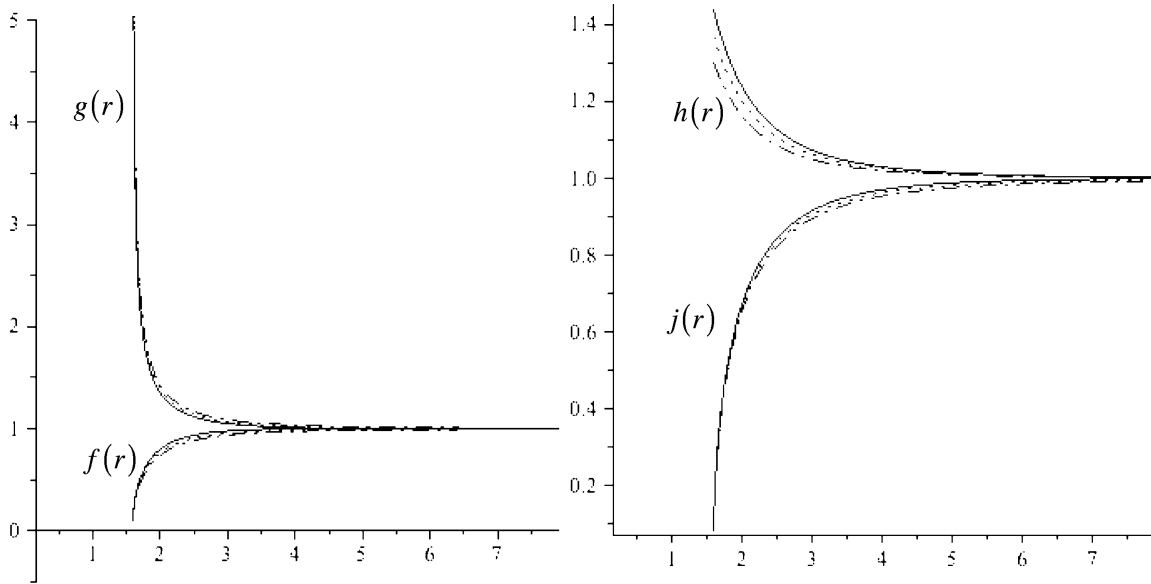


Figure 3: A plot of the metric and gauge functions for $r_0 = 1.6$ for $k = 1$ (solid), $k = 0$ (dot), and $k = -1$ (dot-dash).

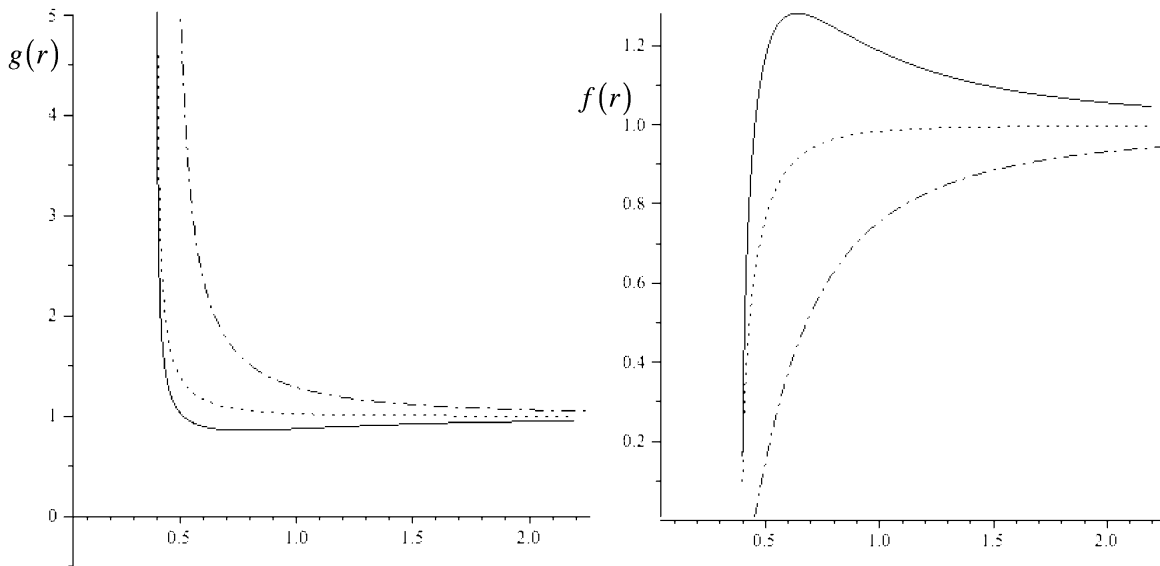


Figure 4: A plot of the metric functions for $r_0 = 0.4$ for $k = 1$ (solid), $k = 0$ (dot), and $k = -1$ (dot-dash).

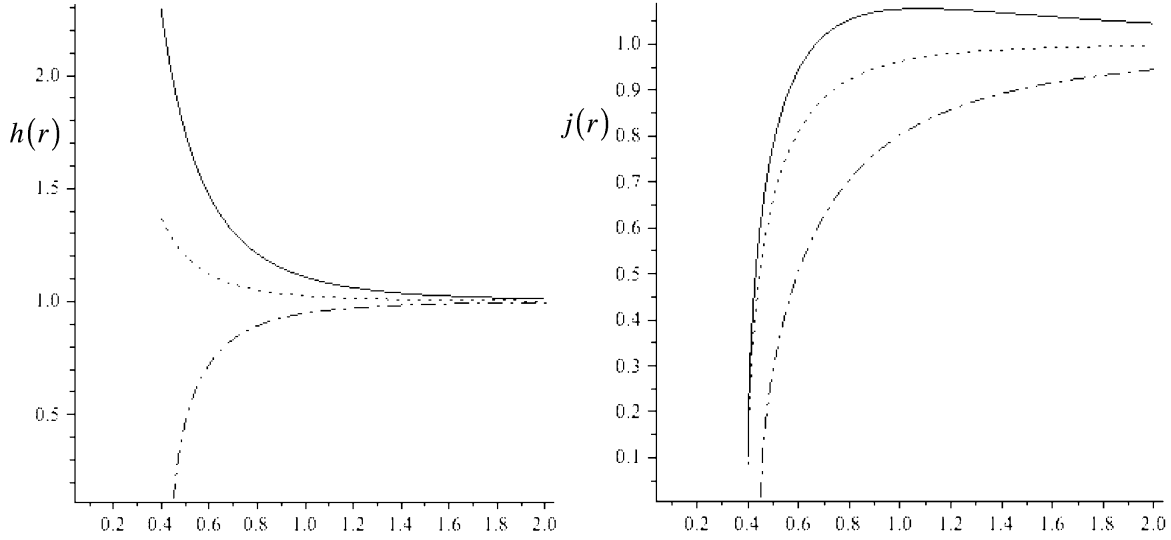


Figure 5: A plot of the gauge functions for $r_0 = 0.4$ for $k = 1$ (solid), $k = 0$ (dot), and $k = -1$ (dot-dash).

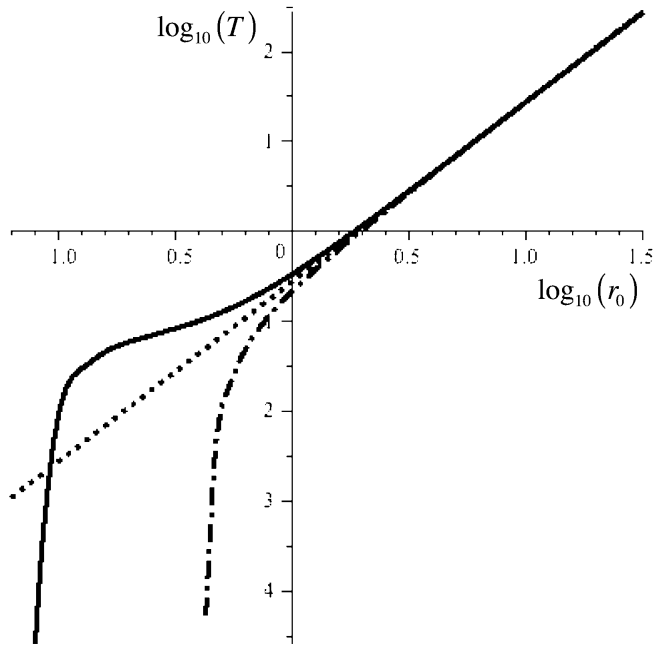


Figure 6: Dependence of the black hole temperature as a function of r_0 for $k = 1$ (solid), $k = 0$ (dot), and $k = -1$ (dot-dash).

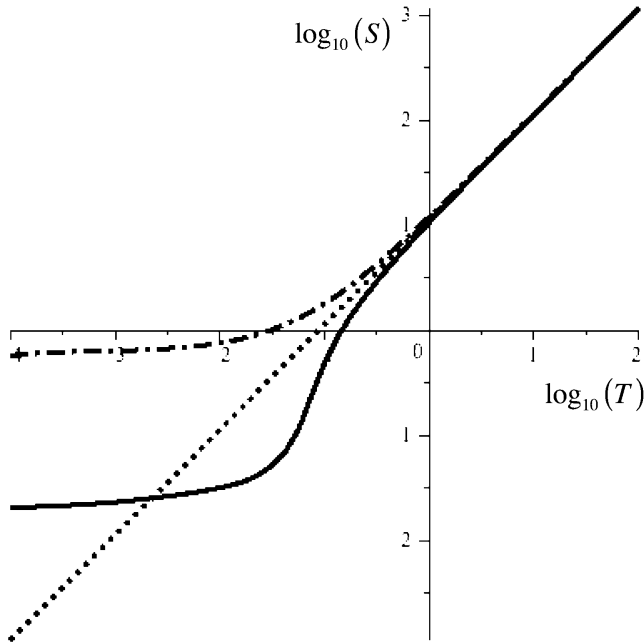


Figure 7: Dependence of the black hole entropy as a function of temperature for $k = 1$ (solid), $k = 0$ (dot), and $k = -1$ (dot-dash).

The temperature for any genus is therefore dependent only on the size r_0 of the black hole, and its behaviour is illustrated in figure 6. For large r_0 , spherical black holes ($k = 1$) are hotter than planar/toroidal black holes ($k = 0$), which are in turn hotter than the $k = -1$ higher genus class. The planar/toroidal holes have a temperature dependence that increases quadratically with the black hole radius; numerically I find that

$$T_{k=0} = 10^{-0.57} r_0^2 = .276 r_0^2 \quad (4.2)$$

a behaviour that also accurately describes the $k = \pm 1$ cases for $r_0 > 0.6$. This behaviour is consistent with the near-horizon expansion that indicates $g_0 \sim 1/f_0 \sim \sqrt{r_0}$ for large r_0 .

For small r_0 the behaviour is strikingly different for each case. Higher genus black holes approach zero temperature at an exponentially rapid rate as $r_0 \rightarrow 1/\sqrt{5}$. For $r_0 < 0.1$ the planar black holes become hotter than their $k = 0$ counterparts. The temperature of the $k = 1$ black holes falls off very rapidly as r_0 decreases, though less so than the $k = -1$ case.

The entropy of the black holes is given by $\frac{1}{4}$ of the area, so $S = \pi r_0^2$ for all cases (assuming appropriate identifications and volume normalizations for $k = 0, -1$). Hence eq. (4.2) gives

$$S = 11.4T \quad (4.3)$$

a relationship that is valid for all T for the $k = 0$ case and that holds for large T for $k = \pm 1$ [11]. The behaviour of the entropy as a function of temperature is given in figure 7.

For the exact solution (2.13), the temperature and entropy are

$$T = \frac{1}{4\pi} \quad S = \frac{\pi}{2} \quad (4.4)$$

which can be computed directly from the exact solution or from the series solution (3.3) for which $f_0 = 1/g_0 = 2^{3/4}$ and $r_0 = 1/\sqrt{2}$. These values are commensurate with those in figure 7, though they are considerably beyond the range for which eq. (4.2) applies.

5 Wilson Loops and the Boundary Dual Theory

Since in (2+1) dimensions one can write $\nabla^2\phi = \vec{\nabla} \times \vec{E}$, where $E_j = \varepsilon_{jk}\nabla^k\phi$, the boundary theory (1.3) can be regarded as a gauge theory in (2+1) dimensions (albeit one with an unusual action) with a dimensionless coupling constant [9, 11]. As in the $k = 0$ spherical case, one can introduce Wilson loops by joining charged particles on the boundary that are connected together in the bulk via a string. The Euclidean action of this string for a rectangular Wilson loop is the same for all values of k and is given by [11, 19]

$$\mathcal{S} = \frac{1}{2\pi\alpha'} \int d\sigma d\tau \sqrt{\det[g_{AB}\partial_\mu X^A\partial_\nu X^B]} = \frac{\Delta\ell^2}{2\pi\alpha'} \int d\theta \sqrt{f^2 r^{2z+2} + f^2 g^2 r^{2z-2} \left(\frac{dr}{d\theta}\right)^2} \quad (5.1)$$

taking $\sigma = \theta$ and $i\tau = t$ in the static gauge, with Euclidean time interval Δ .

Extremizing the action yields a constant of the motion

$$\frac{f^2 r^{2z+2}}{\sqrt{f^2 r^{2z+2} + f^2 g^2 r^{2z-2} \left(\frac{dr}{d\theta}\right)^2}} = f(r_m) r_m^{z+1} \quad (5.2)$$

from which can be computed the boundary length

$$L = \int d\theta = 2 \int_{r_m}^{\infty} \frac{dr}{r^2} \frac{g}{\sqrt{\left(\frac{f}{f_m}\right)^2 \left(\frac{r}{r_m}\right)^{2z+2} - 1}} \quad (5.3)$$

and the regularized potential energy between the two particles

$$V = \frac{\mathcal{S}}{\Delta\ell} = \frac{\ell}{2\pi\alpha'} \left(2 \int_{r_m}^{\infty} dr \frac{r^{z-1} f g}{\sqrt{1 - \left(\frac{f_m}{f}\right)^2 \left(\frac{r_m}{r}\right)^{2z+2}}} - 2 \int_{r_0}^{\infty} dr r^{z-1} f g \right) \quad (5.4)$$

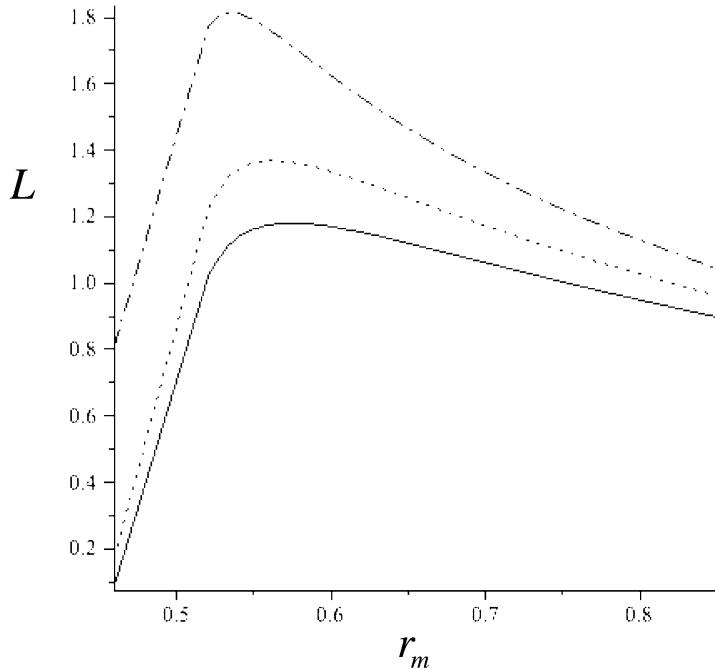


Figure 8: Dependence of the boundary length L between two particles as a function of the string midpoint r_m for $k = 1$ (solid), $k = 0$ (dot), and $k = -1$ (dot-dash), where $r_0 = 0.5$. These curves rapidly become indistinguishable as r_0 increases.

where $f_m = f(r_m)$ and $r_m > r_0$ is the location of the midpoint of the string.

For small r_m the separation L between the particles grows, reaching a maximum and then decreasing as r_m gets larger. The energy between the particles will be negative for sufficiently small r_m , and will vanish at some particular value of r_m (or L). Beyond this point the energy for a single string joining the pair is positive. The energy of the configuration is therefore minimized (to zero) by two (non-interacting) strings stretching from each particle down to the horizon, screening the gauge interaction between the particles. The point at which this takes place will depend on r_0 , and hence the temperature.

For large black holes the metric functions f and g are nearly indistinguishable for all values of k , and so the analysis of screening behaviour for the spherical $k = 0$ case [11] holds for the other values of k as well. For small black holes the value of r_m at which the potential vanishes is numerically almost the same, as in figure 8. However the length between the particles differs considerably as a function of r_m (see figure 9), and so the critical value $L = L_c$ at which screening occurs will differ considerably for different values of k .

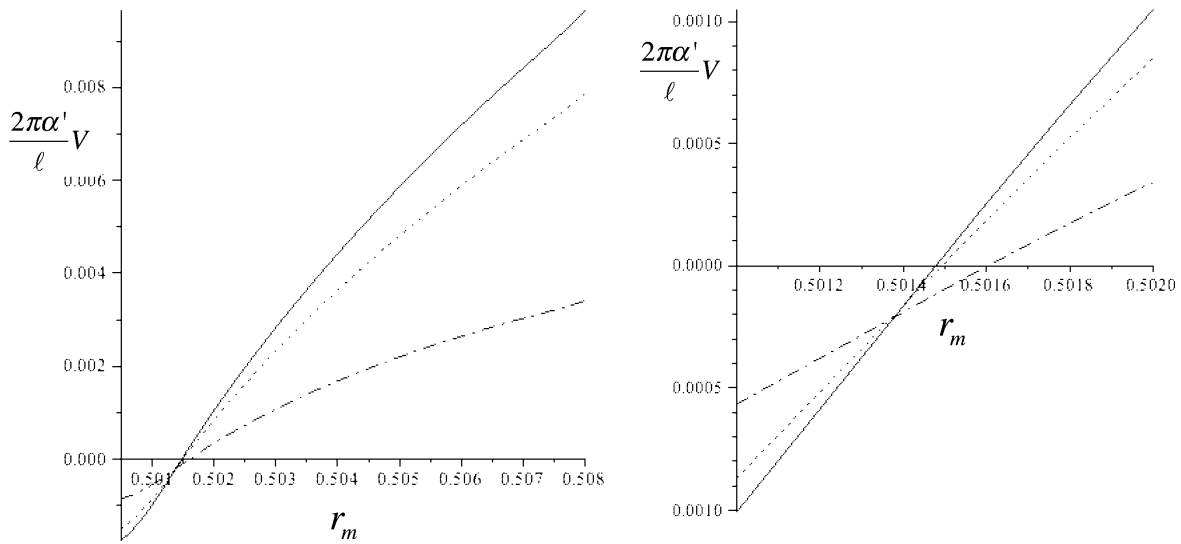


Figure 9: Dependence of the potential V between two particles as a function of the string midpoint r_m for $k = 1$ (solid), $k = 0$ (dot), and $k = -1$ (dot-dash), where $r_0 = 0.5$. The right-hand diagram is a close-up of the left. The critical values of r_m for each k are within 0.04% of each other. The intersection points (and the behaviour of V) rapidly become indistinguishable as r_0 increases.

For the exact solution (2.13) it is straightforward to carry out the integration in equations (5.3) and (5.4), though the results cannot be obtained as an explicit function of r_m but must instead be obtained numerically. It is straightforward to check that the integrands (and hence the integrals) in equations (5.3) and (5.4) are identical within limits of tolerance for the exact solution (2.13) and its numerical counterpart with $r_0 = 1/\sqrt{2}$. The behaviour is not too different for this case as compared to its $k = 0, 1$ counterparts, and so the results are not plotted here.

6 Conclusions

In this paper I have expanded the class of black holes that provide a dual description of a finite temperature a Lifshitz system to include black holes of any topology. The gravitational theory can at least be regarded as a phenomenological description of the 2+1 dimensional physics described by the Lifshitz theory. Whether or not this duality can be fully incorporated into string theory, thereby extending the AdS/CFT correspondence, is an open question.

Thermodynamic properties of these black holes are quite similar for large black holes, but differ considerably for small black holes. The genus 0 and 1 cases approach extremality as the black hole size approaches zero. However the higher-genus black holes approach extremality at $r_0 = 1/\sqrt{5}$, at which point the gauge fields vanish and a negative mass topological AdS black hole is attained.

The screening behaviour of the dual theory is essentially the same for any genus for large black holes. For small black holes the onset of screening is attained at the nearly same value of the midpoint r_m of the string joining two charged particles on the boundary regardless of the genus; however this yields very different values of the critical length L between the particles on the boundary due to a sensitive dependence of this quantity on r_m .

A number of interesting questions remain, including higher-dimensional generalizations, a more complete study of the $z \neq 2$ cases, developing holographic renormalization for this class of theories, and understanding better the relationship with non-relativistic, non-abelian gauge theories having quantum critical behavior at $z = 2$ [20].

Acknowledgements

I am grateful for the hospitality of the Kavli Institute for Theoretical Physics where this work was carried out, and to the Fulbright Foundation and the Natural Sciences and Engineering Research Council of Canada for financial support.

References

- [1] J. M. Maldacena, *The large N limit of superconformal field theories and supergravity*, Adv. Theor. Math. Phys. **2**, 231 (1998) [Int. J. Theor. Phys. **38**, 1113 (1999)]; S. S. Gubser, I. R. Klebanov and A. M. Polyakov, *Gauge theory correlators from non-critical string theory*, Phys. Lett. **B428**, 105 (1998); E. Witten, *Anti-de Sitter space and holography*, Adv. Theor. Math. Phys. **2**, 253 (1998).
- [2] A. Strominger, *The dS / CFT correspondence* JHEP **0110** 034 (2001); V. Balasubramanian, J. de Boer and D. Minic, *Mass, entropy and holography in asymptotically de Sitter spaces*, Phys.Rev. **D65** 123508 (2002); A.M. Ghezelbash and R.B. Mann, *Action, mass and entropy of Schwarzschild-de Sitter black holes and the de Sitter / CFT correspondence* JHEP **0201** 005 (2002).
- [3] R. B. Mann and D. Marolf, “Holographic renormalization of asymptotically flat spacetimes,” Class. Quant. Grav. **23**, 2927 (2006); D. Marolf, *Asymptotic flatness, little string theory, and holography* JHEP **0703** 122 (2007); R. B. Mann, D. Marolf, R. McNees and A. Virmani *On the Stress Tensor for Asymptotically Flat Gravity* Class. Quant. Grav. **25** 225019 (2008).
- [4] P. Kovtun, D. T. Son, and A. O. Starinets, *Viscosity in strongly interacting quantum field theories from black hole physics* Phys. Rev. Lett. **94** 111601 (2005).
- [5] S. A. Hartnoll, C. P. Herzog and G. T. Horowitz, *Building a Holographic Superconductor* Phys. Rev. Lett. **101** 031601 (2008).
- [6] S. A. Hartnoll and P. Kovtun, *Hall conductivity from dyonic black holes* Phys. Rev. **D76** 066001 (2007)
- [7] S. A. Hartnoll, *Lectures on holographic methods for condensed matter physics* [e-Print: arXiv:0903.3246].

- [8] D.S. Rokhsar and S.A. Kivelson, *Superconductivity and the Quantum Hard-Core Dimer Gas* Phys. Rev. Lett. **61** 2376 (1988); E. Ardonne, P. Fendley and E. Fradkin, *Topological order and conformal quantum critical points* Annals Phys. **310** 493 (2004); E. Fradkin, D.A. Huse, R. Moessner, V. Oganesyan, and S.L. Sondhi, *Bipartite Rokhsar-Kivelson points and Cantor deconfinement* Phys. Rev. **B69** 224415 (2004).
- [9] A. Vishwanath, L. Balents, and T. Senthil, *Quantum Criticality and Deconfinement in Phase Transitions Between Valence Bond Solids* Phys. Rev. **B69** 224416 (2004).
- [10] S. Kachru, X. Liu, and M. Mulligan, *Gravity Duals of Lifshitz-like Fixed Points* Phys. Rev. **D78** 106005 (2008).
- [11] U. H. Danielsson and L. Thorlacius *Black holes in asymptotically Lifshitz spacetime* JHEP **0903** 070 (2009).
- [12] J. P. S. Lemos, *Cylindrical black hole in general relativity* Phys. Lett. B353 46 (1995); S. Aminneborg, I. Bengtsson, S. Holst, P. Peldan *Making anti-de Sitter black holes* Class. Quant. Grav. **13** 2707 (1996); R. G. Cai and Y. Z. Zhang, *Black plane solutions in four dimensional spacetimes* Phys. Rev. D54 4891 (1996); R.B. Mann *Pair production of topological anti-de Sitter black holes* Class. Quant. Grav. 14 L109 (1997); D.R. Brill, J. Louko and P. Peldan *Thermodynamics of (3+1)-dimensional black holes with toroidal or higher genus horizons* Phys.Rev. **D56** 3600 (1997);
- [13] R.B. Mann *Black Holes of Negative Mass* Class. Quant. Grav. **14** 2927 (1997).
- [14] C. P. Herzog, M. Rangamani and S. F. Ross, *Heating up Galilean holography* JHEP **0811**, 080 (2008); J. Maldacena, D. Martelli and Y. Tachikawa, *Comments on string theory backgrounds with non-relativistic conformal symmetry* JHEP **0810** 072 (2008); A. Adams, K. Balasubramanian and J. McGreevy, *Hot Spacetimes for Cold Atoms* JHEP **0811** 059 (2008); P. Kovtun and D. Nickel, *Black holes and non-relativistic quantum systems* arXiv:0809.2020 [hep-th]; P. Horava, *Quantum Gravity at a Lifshitz Point* arXiv:0901.3775 [hep-th].
- [15] D. Yamada, *Thermodynamics of Black Holes in Schroedinger Space* arXiv:0809.4928 [hep-th]; R.B. Mann *Solitonic Phase Transitions of Galilean Black Holes* arXiv:0903.4228 [hep-th]; R.G. Cai, L.M. Cao and N. Ohta *Topological Black Holes in Horava-Lifshitz Gravity* e-Print: arXiv:0904.3670

- [16] R.B. Mann and W. Smith, *Formation of topological black holes from Gravitational Collapse* Phys.Rev. **D56** 4942 (1997).
- [17] R.B. Mann *Topological black holes: Outside looking In*, in *Internal structure of black holes and spacetime singularities*, pg. 311 eds. L. Burko and A. Ori, (Technion Press, 1998).
- [18] G.T. Horowitz and S.F. Ross, *Naked Black Holes* Phys. Rev. **D56** 2180 (1997); I.S. Booth and R.B. Mann *Static and infalling quasilocal energy of charged and naked black holes* Phys.Rev. **D60** 124009 (1999).
- [19] J. M. Maldacena *Wilson loops in large N Field theories* Phys. Rev. Lett. **80** 4859 (1998); S. J. Rey and J. T. Yee, *Macroscopic strings as heavy quarks in large N gauge theory and anti-de Sitter supergravity* Eur. Phys. J. **C22** 379 (2001).
- [20] P. Horava, *Quantum Criticality and Yang-Mills Gauge Theory* arXiv:0811.2217 [hep-th].